Artigos técnicos

Effect of Particle Geometry and Nb_2O_5 Addition in the Sintering of Partially Stabilized Zirconia with Y_2O_3

Catia Fredericci[a*], Alexandre M. Jordão[b], Arnaldo M. Shima Junior[b], Fernanda C.P. Baraldini[b], Flávio I. Santana[b], Juliana I. Affonso[b], Laércio A. Piva[b], Liece Rodrigues Junior[b], Pedro Garcia[b], Juliana Flor[c]

a Laboratório de Processos Metalúrgicos, Instituto de Pesquisas Tecnológicas do Estado de São Paulo S.A., São Paulo-SP, Brasil.
b Programa de Pós-Graduação do IPT em Processos Industriais
c Fundação de Apoio ao IPT, São Paulo-SP, Brasil.

*E-mail: catiaf@ipt.br

Keywords:
sintering; ZrO_2, Nb_2O_5; spray dryer; powders

Abstract

Zirconia (ZrO_2) has several applications in diverse industrial segments due to its excellent properties, especially regarding resistance to mechanical stress and high-temperature scenarios. However, due to phase transformations that this ceramic material exhibits at various temperatures, the appearance of cracks in the sintered compact during cooling is perceived. Studies have been performed in the way to stabilize zirconia during the sintering process by adding small quantities of other oxides, such as Y_2O_3, CeO, MgO and Nb_2O_5. Some studies show that the use of Nb_2O_5 in the system ZrO_2-Y_2O_3 promotes an increase in its fracture toughness. Additionally, there are several controversies about the effect of the content and the polymorph of Nb_2O_5 on zirconia stabilization. There are several commercial zirconia powders partially stabilized in the form of granules obtained by the spray dryer method which promotes better densification of the green and sintered compacts. This study aims at evaluating the effect of adding 0.8 % and 2.0 % (by weight) of monoclinic Nb_2O_5 in 3Y-TZ-E (Tosoh) on the stabilization of this zirconia and the grinding effect of 3Y-TZ-E granules on the densification and on the sintered compact microstructure. Sintered compacts were characterized by X-ray diffraction, scanning electron microscopy, and Raman spectroscopy. The results indicate that

the use of 2.0 % (in weight) of Nb_2O5 implies in the destabilization of tetragonal zirconia and in the formation of $Zr_6Nb_2O_{17}$. No significant difference was observed in the densification and in the grain size of the unground TZ-3Y-E with the addition of 0.8 % (in weight) of monoclinic Nb_2O_5.

1 Introduction

Zirconia is one of the most important oxides due to its large diversity of applications, ranging from fuel cells, thermal barrier protection, impact-resistant materials, burner blocks, biomaterials such as hip and dental implants (YOSHIMURA et al., 2007), and so on. The zirconia appears in three polymorphic forms such as monoclinic (m), tetragonal (t) and cubic (c), depending on the temperature: monoclinic m-ZrO_2 up to 1100 °C, t-ZrO_2 up to 2285 °C, and c-ZrO_2 above this temperature (RODDATIS et al., 2002). During cooling, the tetragonal phase becomes the monoclinic followed by large volume variation (3 % to 5 %) which is enough to fracture a sintered compact (YOSHIMURA et al., 2007). Gupta et al. (1977, 1978) reported that it is possible to manufacture dense monolithic zirconia compacts with small grain size (~ 0.3 µm) containing approximately 98 % of tetragonal phase with the addition of small portions of Y_2O_3 for metastable phase retention. Other oxides such as CaO, MgO, and rare-earth oxides can be used for zirconia stabilization (BEJUGAMA; PANDEY, 2018). Also according to Gupta et al. (1977), zirconia-based ceramics with metastable phase present high toughness ((6 to 9) MNm-3/2 = (6 to 9) MPa.m1/2), when compared to other ceramics such as alumina (4 MNm-3/2) and monocrystalline spinel (1.3 MNm-3/2), for example.

Same as zirconia, niobium pentoxide (Nb_2O_5) is also found in several polymorphic forms such as TT and T (low temperatures), M and B (average temperatures) and H (high temperatures). The most common polymorphs are T-Nb_2O_5 and H-Nb_2O_5, orthorhombic and monoclinic, respectively. According to Piralek, Pelczarska and Szczygiel (2017), phase H is thermodynamically more stable and can be obtained from any polymorph from heat treatment. These authors studied the niobium pentoxide polymorphic transformations, including the optical grade (CBMM), and reported that at ambient temperature this raw material is composed of phases T, H and M, and after heat treatments above 900 °C the tetragonal phase disappears, and phase H (monoclinic) becomes predominant after cooling. Guha (1969) also reported that two polymorphs were observed in Nb_2O_5, namely, a low temperature form that turns irreversibly in the form of high temperature at about 850 °C. Nb_2O_5 monoclinic, once formed, becomes stable throughout the process and therefore is the equilibrium phase at all temperatures above the ambient one.

Small partially stabilized zirconia particles, when dispersed in a matrix, can increase its toughness. This is due to monoclinic-tetragonal transformation, causing compressive residual stress, closing the crack tips present in the matrix (CALLISTER, 2016).

Efforts are being dedicated in attempts to increase fracture toughness of Nb_2O_5-ZrO_2 system. Jin, Gao and Kan (2002), for example, studied the effect on t-ZrO_2 toughening in mullite ($3Al_2O_3$. $2SiO_2$) and reported that although the addition of Nb_2O_5 in ZrO_2 makes the tetragonal phase more unstable, it resulted in an increase in m-ZrO_2 phase, and mechanical properties have been considerably improved. Golieskardi, Satgunam and Ragurajan (2014) developed a two-step method of treatment aiming at increasing ceramic density by reducing grain size at the final sintering stage. Increasing density, mechanical properties such as hardness, toughness and attrition resistance have improved considerably. The authors reported that several researchers studied the effect of the addition of CeO_2, MgO, Al_2O_3 and Nb_2O_5 as sintering aids in the Y-TZP (yttria-stabilized tetragonal zirconia polycrystalline) to improve ceramics properties and microstructure control, such as Kimura et al. (1988), Ramesh (2001), Hwang and Chen (1990) and Ran et al. (2007). Golieskardi, Satgunam and Ragurajan (2014) obtained ceramics from the TZP-Nb_2O_5 system with approximately 97 % densification at 1500 °C with a maximum of 1 % (by weight) of Nb_2O_5 and fracture toughness of 8.5 MPam1/2. Kim (1990) studied the effect of adding Ta_2O_5, Nb_2O_5 and HfO_2 on the transformation of ZrO_2 stabilized with yttria (2Y-TZP and 3Y-TZP). The powders were prepared by the coprecipitation method with Nb_2O_5 ratios of 0.0 %, 0.5 %, 1.0 % and 1.5 % in mol (between 0.0 wt% and 3.0 wt %). The authors have prepared specimens from isostatic pressing with 170 MPa and sintering treatment at 1500 °C for 1 . The density of the samples was ≥ 97 % of the theoretical density. In another work of Kim et al. (1998), the authors had studied the effect of adding 0.0 %, 0.5 %, 1.0 % 0 and 1.5 % Nb_2O_5 (in mol) in 3Y-TZP (Tosoh). The Nb_2O_5 brand and polymorph were not disclosed. The authors mention that all samples presented only the t-ZrO_2 phase and that when more than 1.5 % (mol) of Nb_2O_5 was added, it became difficult to obtain pure tetragonal phase, resulting in destabilization of yttria stabilized zirconia.

As a critical topic, authors noted that in many references, polymorphic phases for both zirconia and niobium pentoxide are not specified (LOPES et al., 2015; GUHA, 1969).

Another important topic in ceramic materials processing is that the geometry and particle size distribution influence the pressing and sintering processes. Granulated powders, obtained by spray dryer method, present greater fluidity and, therefore, easiness and homogeneity in filling the mold (SANTANA et al., 2008). Thus, the closer and more compact the raw materials particles are, the greater the compaction of the green compact will be and the better the sinterability of the material, increasing densification, which is critical for applications that demand high mechanical strength.

According to Brito, Medeiros and Lourenço (2007), sintering corresponds to the physical process where compressed powders are subjected to high temperatures (slightly below their melting point) so that they acquire mechanical resistance. In this process, the porosity is decreased as a consequence of the decrease of free surface energy on the particle compact, by reducing the total surface of the system. That results in total or partially dense body.

This works aims at studying the effect of the addition of the monoclinic Nb_2O_5 on the stabilization of TZ-3Y (Tosoh) and at studying the effect of the particles geometry on the microstructure of the sintered compact in the system TZ-3Y-Nb_2O_5.

2 Experimental Procedure

This section presents the raw materials used, their characterization and the method of preparation of green and sintered compacts.

2.1 Materials

The following raw materials were used: TZ-3Y-E from Tosoh Corporation (as received – without grinding), TZ-3Y-E from Tosoh Corporation, ground in a mortar and sieved on a sieve of 270 mesh and Nb_2O_5 optical grade of CBMM (Table 1), treated to 1000 °C for 3 h, for obtaining only the monoclinic phase. TZ-3Y-E already features binders, facilitating the molding of the green compact. As the Nb_2O_5 presents very coarse-grained aggregates (> 20 µm), making homogenization difficult in zirconia, wet grinding in a planetary mill was required. The milling process was carried out in a Pulverizette 5 Fritsch mill for 2 h, using 20 g of monoclinic Nb_2O_5, 50 mL of isopropyl alcohol and 100 g of zirconia balls of approximately 10.8 mm at 150 rpm, in order to obtain a fine niobium pentoxide powder to promote better homogenization between the two oxides (ZrO_2 + Nb_2O_5).

Table 1 – Characteristics of used powders: TZ-3Y-E and Nb_2O_5

Raw Material	TZ-3Y-E	Nb_2O_5
Supplier/Manufacturer	Tosoh	CBMM
Condition	Commercial	Commercial
Category	5.2 % (weight) Y_2O_3 (3 % mol)	Optical grade
Density (g/cm³)	6.05	4.6

Source: created by authors

2.2 Specimens Preparation

The raw materials were mixed according to the ratios of 0.0 % wt, 0.8 % w (0.37 % mol) and 2.0 % wt (0.93 % mol) of monoclinic Nb_2O_5 (Table 2) in ball mill without any grinding element for 8 h in order to not compromise the granular shape of TZ-3Y-E, generating then samples ZS0.0, ZS0.8, ZS2.0. The ground TZ–3Y–E sample with addition of 0.8 % wt was named ZM0.8, as described in Table 2. After that, the mixtures were dried at 100 °C in an oven for 14 h.

Table 2 – Studied Compositions

wt%	*mol%*	*Samples*
TZ–3Y–E unground + 0.0 Nb_2O_5	TZ–3Y-E unground + 0.0 Nb_2O_5	ZS0.0
TZ–3Y-E unground + 0.8 Nb_2O_5	TZ–3Y–E unground + 0.37 Nb_2O_5	ZS0.8
TZ–3Y-E unground + 2.0 Nb_2O_5	TZ–3Y-E unground + 0.93 Nb_2O_5	ZS2.0
TZ–3Y-E ground + 0.8 Nb_2O_5	TZ–3Y-E ground + 0.37 Nb_2O_5	ZM0.8

Source: created by authors

Specimens in the disk form were prepared in a mold with a diameter of 11.36 mm. Approximately one gram of the compositions (Table 2) was pressed uniaxially by 200 MPa in an EMIC machine (model DL 10000). The pressing method was chosen based on Lopes (2009).

The specimens were sintered in a Fortlab oven with the following heating rates: from room temperature to 800 °C at 8 °C/min, from 800 °C to 1200 °C at 5 °C/min and from 1200 °C to 1500 °C at 3 °C/min.

2.3 Characterizations

2.3.1 X-ray diffraction

Raw materials and sintered samples were characterized by X-ray diffraction using the Shimadzu DRX 6000 equipment, $K_{\alpha}Co$ radiation, scanning of 1° per minute, to determine crystalline phases.

2.3.2 Scanning Electron Microscopy

The scanning electron microscope (SEM) used was the FEG Quanta 3D (with an acceleration voltage of 20 kV) to check the powders´ particle sizes and the microstructure of the green and sintered compacts.

The grain size of the sintered compacts was measured from SEM images using the Scandium (Olympus) software. At least 100 grains of three micrographs of each specimen were measured.

2.3.3 Raman Spectroscopy

As the Nb_2O_5 content was a maximum of 2 % w (0.93 % mol), it was not possible to identify it by X-ray diffraction. Therefore, Raman spectroscopy was used. Raman is a technique which allows analyzing several specific regions in the sample since the diameter of the laser is approximately 2 µm.

Raman spectra were obtained from the surface of the sample ZS2.0, using Raman Confocal spectrophotometer WiTec alpha 500, containing double monochromator, 600 lines/mm and a CCD detector. The focusing of the laser on the sample and collection scattered radiation at 180° were done by a WiTec metallurgical microscope and objective lens of 100x CF Plan aperture number of 0.55. An excitation line in the visible region was used at 532 nm of Argon laser (WiTec brand, S/N 100-1665-154). The laser power was kept below 20 mW. Each spectrum corresponds to the average of 100 accumulations, acquired with an integration time of 50 s.

2.3.4 Green and Sintered Specimens' Density Measurement

Green specimen density (p) was measured for determining the compaction level. These measurements were performed with a Mitutoyo digital caliper, measuring the diameter and height of each specimen. The volume was calculated according to the expression $v = \pi r^2 h$. *The samples were weighed and the expression* $p = m/v$ *was used to calculate the green specimen density. The density (p) for the densification percentage calculation was theoretical, using the value of 6.05 g/cm³ of TZ-3Y-E, provided by the manufacturer and 4.6 g/cm³ for monoclinic niobium pentoxide, using the mixture method:* $pmixture = 1/Mass_{ZrO2}/p_{ZrO2} + 1/MassNb_2O_5/pNb_2O_5$. *The value used for calculations was 6.0 g/cm³ when using 0.8 % wt of* Nb_2O_5. *The values related to the samples with 2 % wt of* Nb_2O_5 *were not calculated for reasons presented in the results and discussion section.*

The sintered specimens were characterized by apparent density using the Archimedes method (Equation 1).

$$D_{ap} = (M_s/M_s - M_i) \times p_{water} \quad (1)$$

where D_{ap} *= apparent density,* m_s *= dry mass and* m_i *= immersed mass. The temperature was 18 °C and* p_{water} *(water density) was considered 0.9986, according to Haynes (2014). Five specimens of each composition were analyzed and the result was expressed as an avarage values and an standard deviation.*

3 Results and Discussions

In this section, results and discussions regarding the raw materials and green and sintered specimens are described.

3.1 Raw materials

As shown in Figure 1, the niobium pentoxide (optical grade) provided by CBMM presents orthorhombic (T) and monoclinic (H) phases. The M phase, identified by Piralek, Pelczarska and Szczygiel (2017), for the Nb_2O_5 optical grade, was not found in this work. The heat treatment performed at 1000 °C for 3 h resulted in the monoclinic Nb_2O_5 as can be seen in Figure 1.

Figure 1 – X-ray diffractograms of the samples: Nb_2O_5 CBMM (optical grade) as received and processed at 1000 °C for 3 h

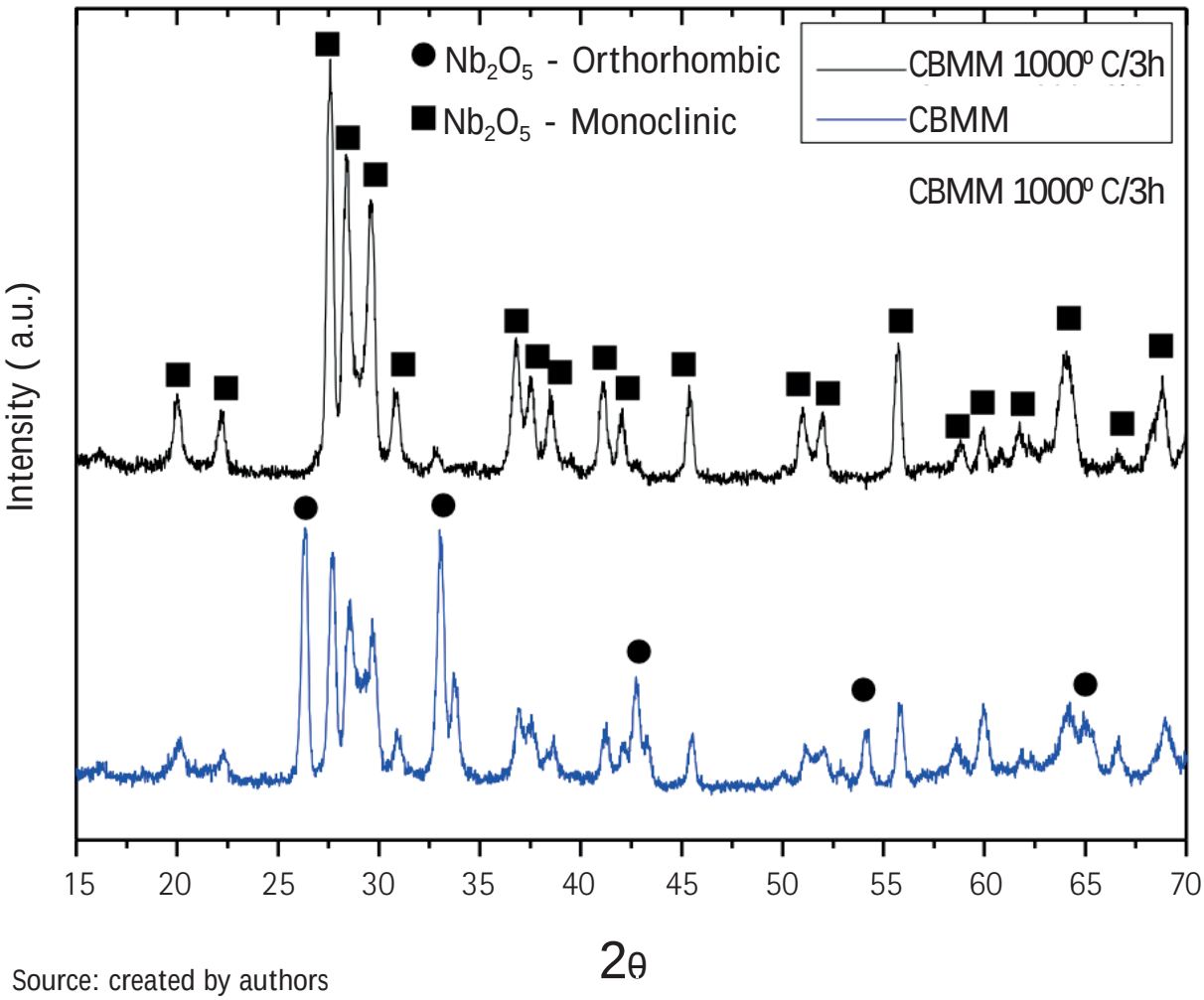

Source: created by authors

Regarding zirconia TZ-3Y, the X-ray diffractogram (Figure 2) shows a monoclinic phase (smaller quantity) and the mostly tetragonal phase.

Figure 2 – X-ray diffractogram of TZ-3Y-E Tosoh sample

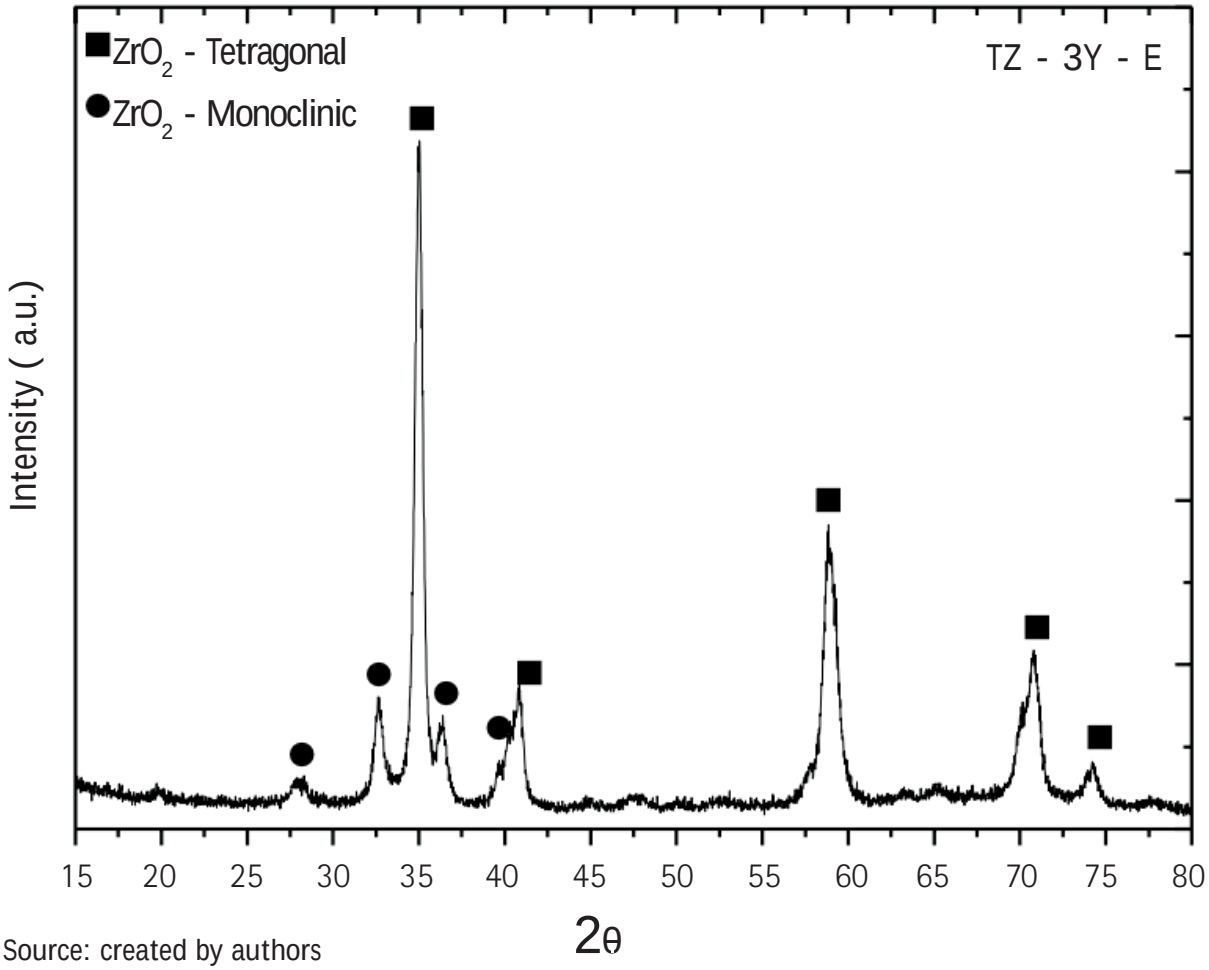

Source: created by authors

Figure 3 shows micrographs obtained by scanning electron microscopy (SEM) of TZ-3Y-E and Nb_2O_5 powders (optical grade) processed by 1000 °C for 3 h and ground by planetary mill, as described on section 2.1. Nb_2O_5 powder has presented aggregates greater than 20 µm (Figure 3b). As small quantities of it were mixed with TZ-3Y-E the milling process was necessary to promote the best homogenization of the powders.

3.2 Relative Density of Green Specimens

The apparent density is the ratio between the mass of a sample and its volume, including the contribution of the empty volume between particles. The apparent density values were converted into relative density, considering the density of ZS0.0 as 6.1 g/cm³ and the ZS0.8 sample as 6.0 g/cm³. Figure 4 shows the relative density for the green compacts. ZS0.0 and ZS0.8 samples have higher green densification (~48 %) in relation to the ZM0.8 sample (~ 46 %) indicating that the particle morphology in the form of granule results in better packaging of the green compact ZS0.8, in a scale of 4 % higher compared to ZM0.8.

Figure 3 – Micrographs obtained by SEM: (a) TZ-3Y-E as received, (b) Nb_2O_5 treated at 1000 ºC for 3 h, (c) and (d) milled Nb_2O_5 (monoclinic)

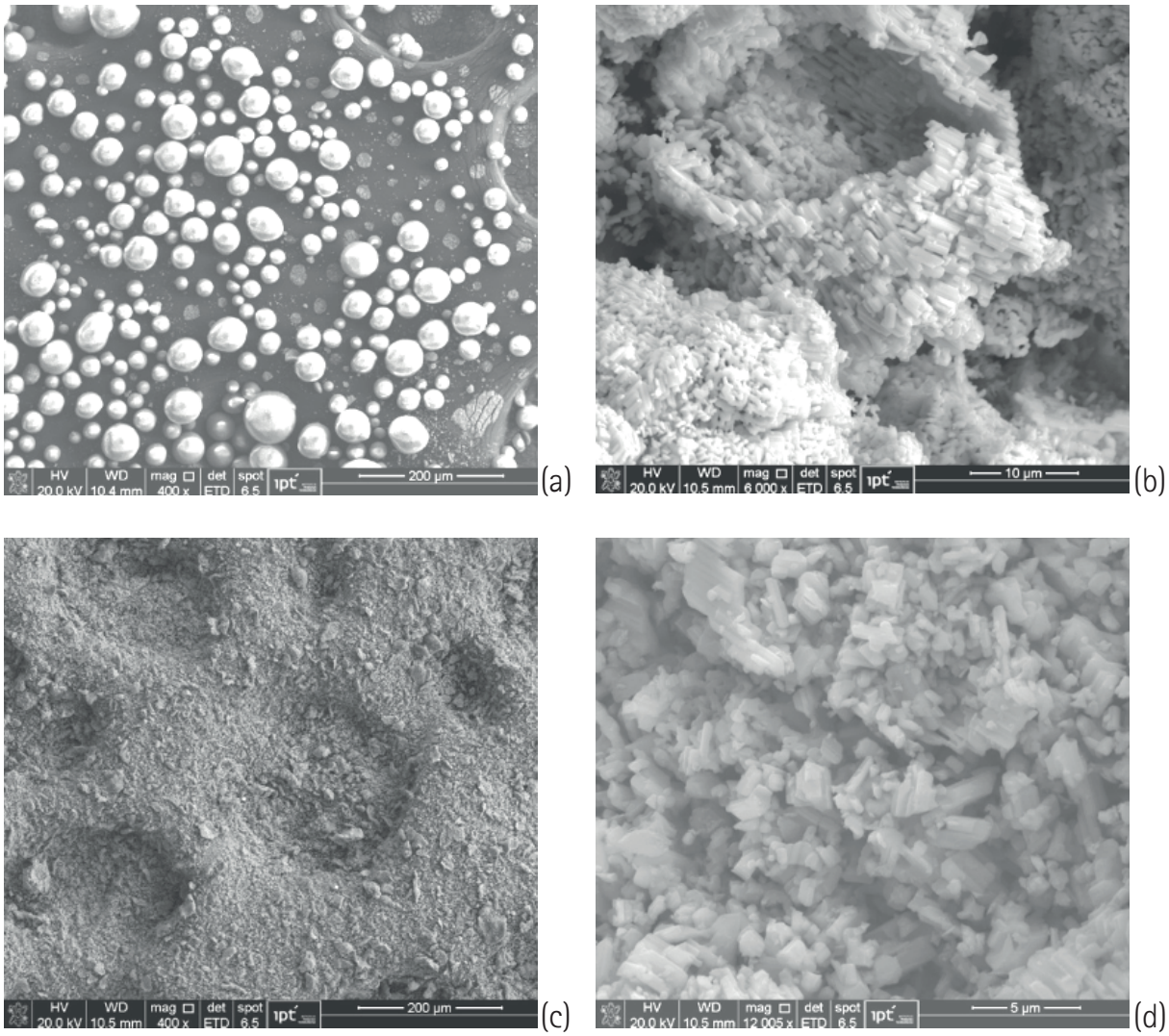

Source: created by authors

Figure 4 – Relative density of uniaxially compacted powders (green compacts – before sintering)

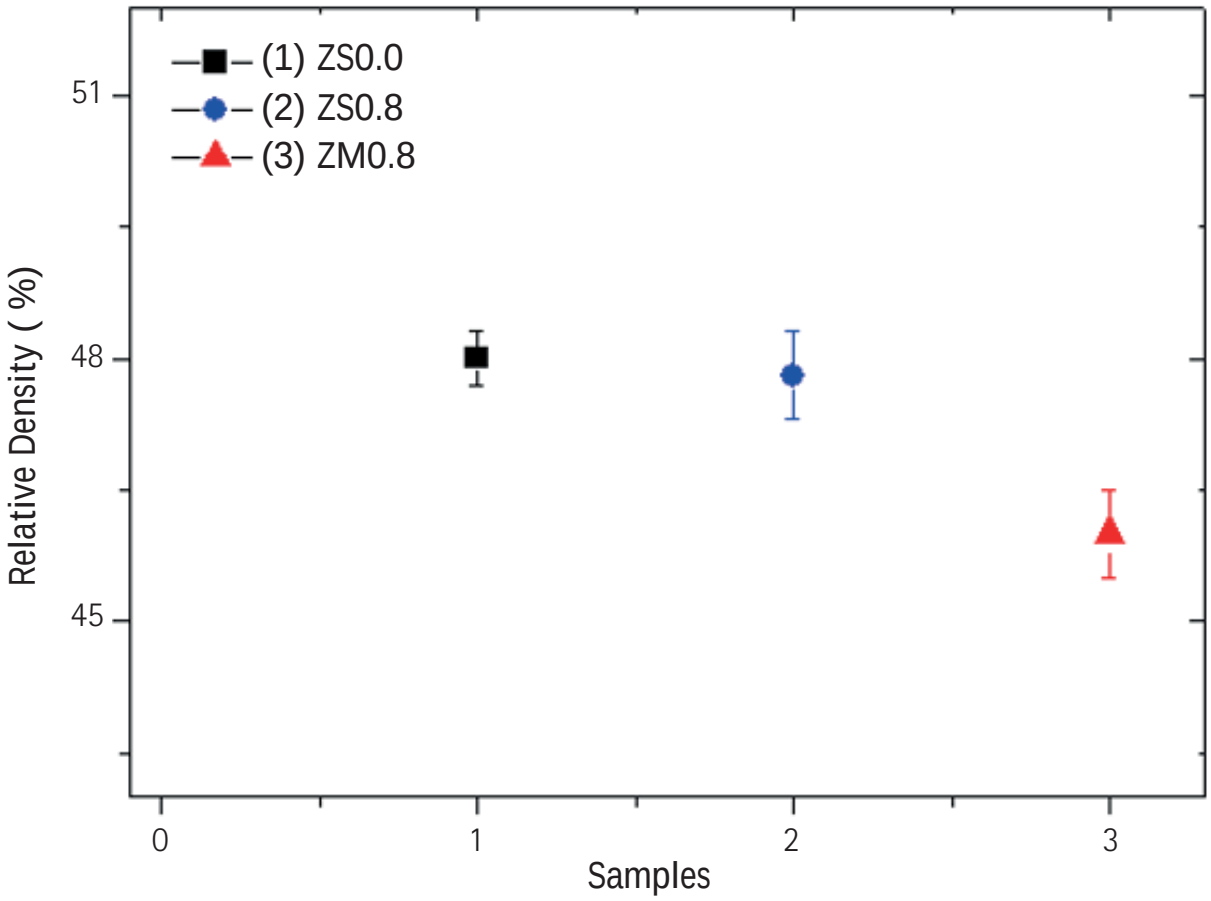

Source: created by authors

Figure 5 shows that green compacts ZS0.0 and ZS0.8 present some granules, as pointed by arrows in Figures 5a to 5d; others were destroyed by pressing. In the ground TZ-3Y-E sample mixed with 0.8 % wt Nb_2O_5 (ZM0.8), the granules are not observed.

Figure 5 – Micrographs obtained by SEM: (a) and (b) of the green compact ZS0.0, (c) and (d) of the green compact ZS0.8, (e) and (f) of the green compact ZM0.8.

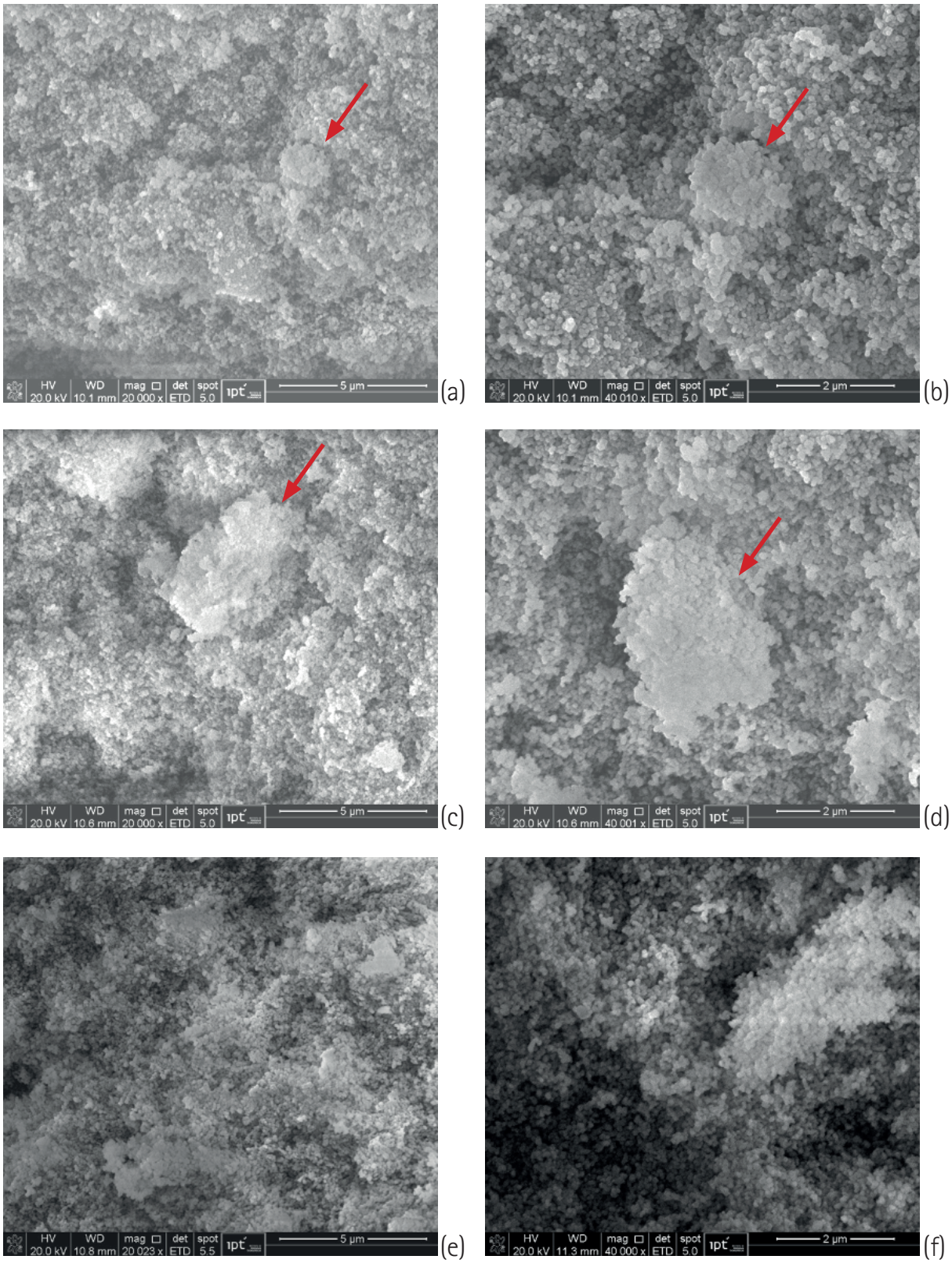

Source: created by authors

3.3 Characterization of Sintered Compacts

3.3.1 Densification and Scanning Electron Microscopy Analyses

Figure 6 presents the relative density of the ZS0.0, ZS0.8 and ZM0.8 sintered compacts. It was not possible to measure the density of the sintered compacts with the addition of 2 % wt of Nb_2O_5, due to the high quantity of cracks resulting in fragmentation when handling the samples (Figure 7).

Figure 6 – Relative density of ZS0.0, ZS0.8 and ZM0.8 sintered compacts

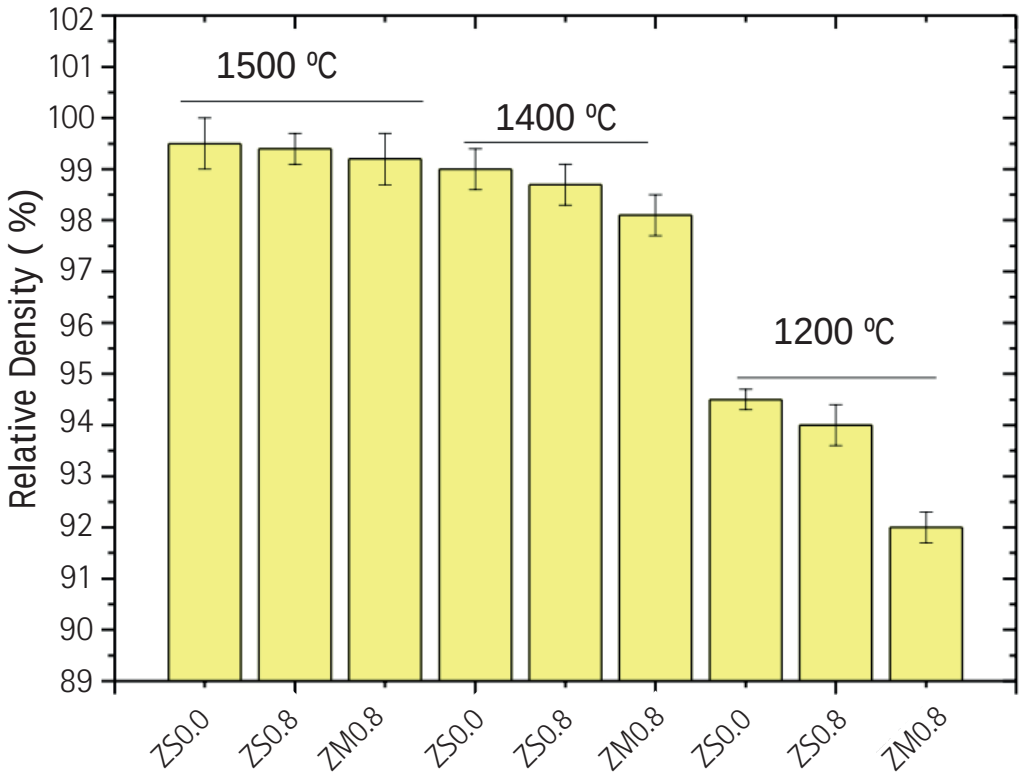

Source: created by authors

Figure 7 – Images of compacts sintered at 1400 ºC for 3 h: (a) ZS2.0 and (b) ZS0.8

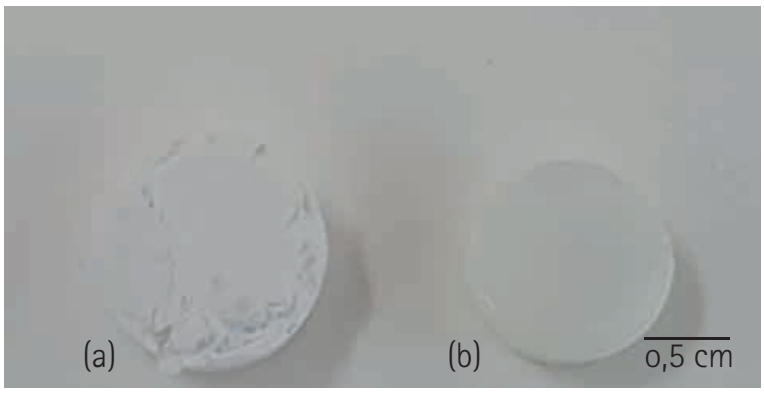

Source: created by authors

Figures 8, 9 and 10 show scanning electronic micrographs of the fractured and polished surface of the sintered compacts at 1200 °C, 1400 °C and 1500 °C for 3 h, respectively.

Figure 8 – Micrographs obtained by SEM of the specimens treated at 1200 ºC for 3 h
(left side: fractured surface TZ-3Y-E and right side: polished surface)

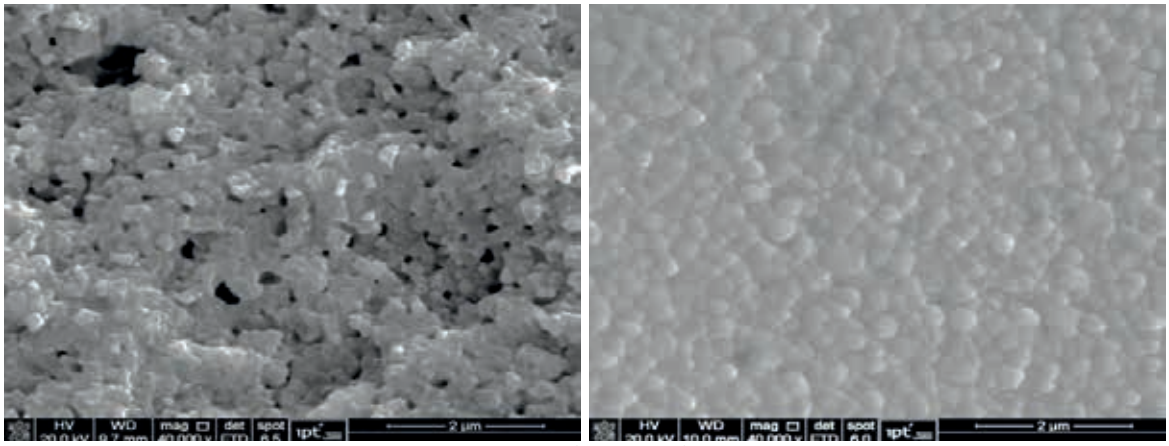

(a) ZS0.0 (1200 °C)

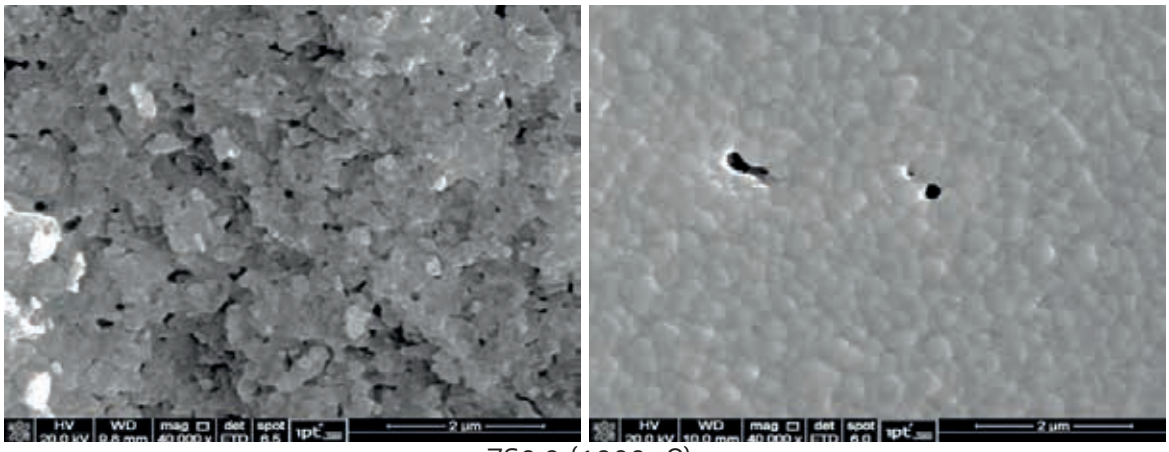

(b) ZS0.8 (1200 °C)

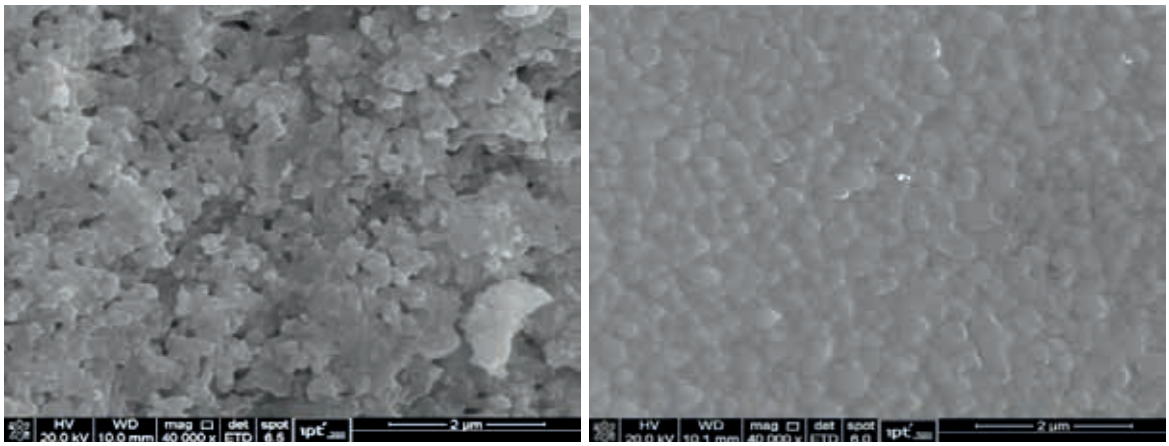

(c) ZM0.8 (1200 °C)

Source: created by authors

Figure 9 – Micrographs obtained by SEM of the specimens treated at 1400 ºC for 3 h (left side: fractured surface TZ-3Y-E and right side: polished surface)

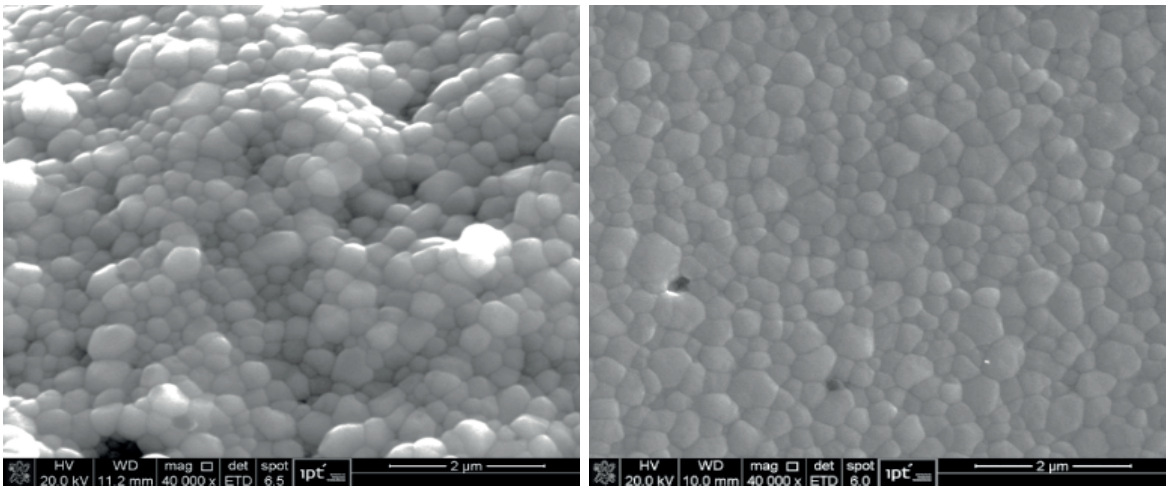

(a)

ZS0.0 (1400 ºC)

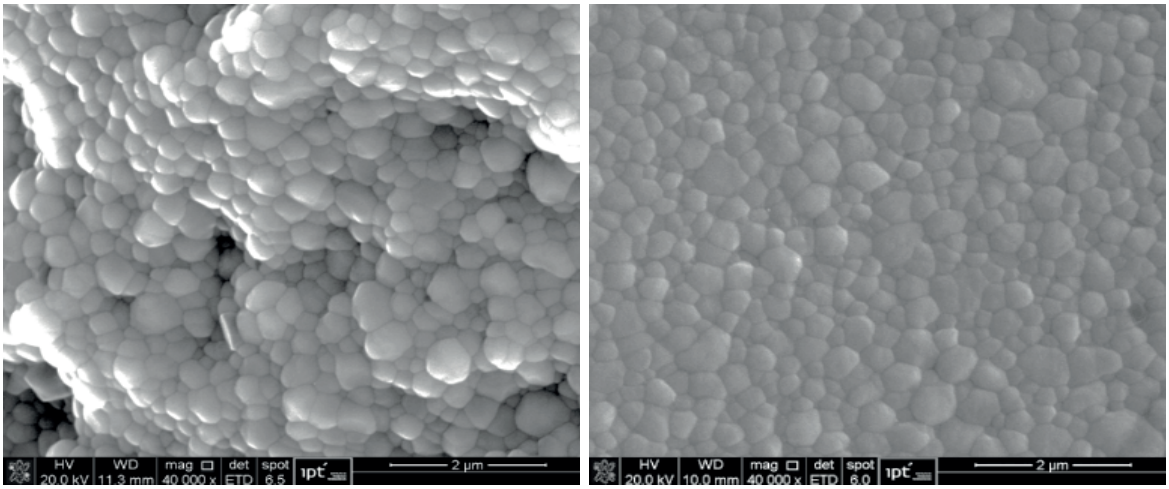

(b)

ZS0.8 (1400 ºC)

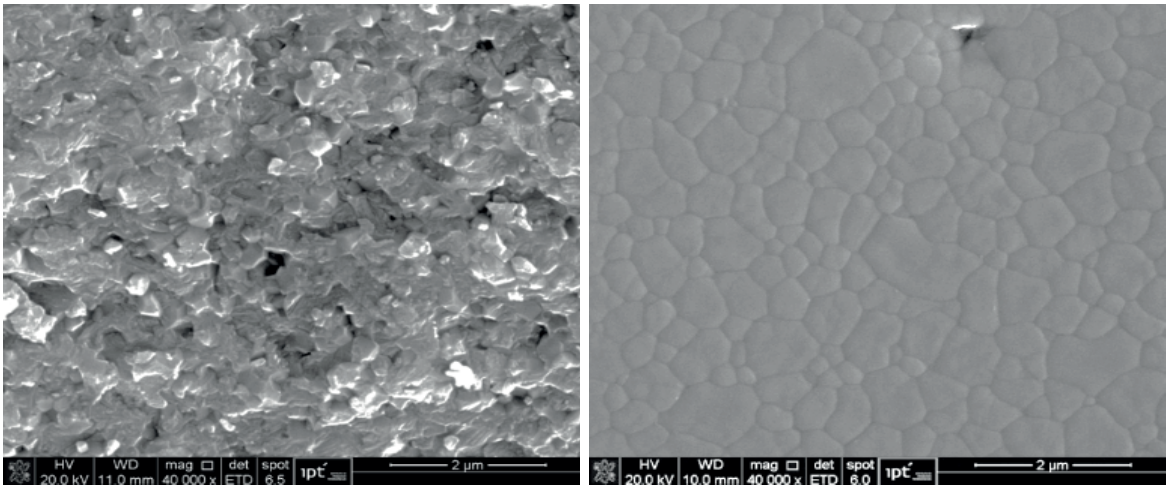

(c)

ZM0.8 (1400 ºC)

Source: created by authors

Figure 10 – Micrographs obtained by SEM of the specimens treated at 1500 ºC for 3 h
(left side: fractured surface TZ-3Y-E and right side: polished surface)

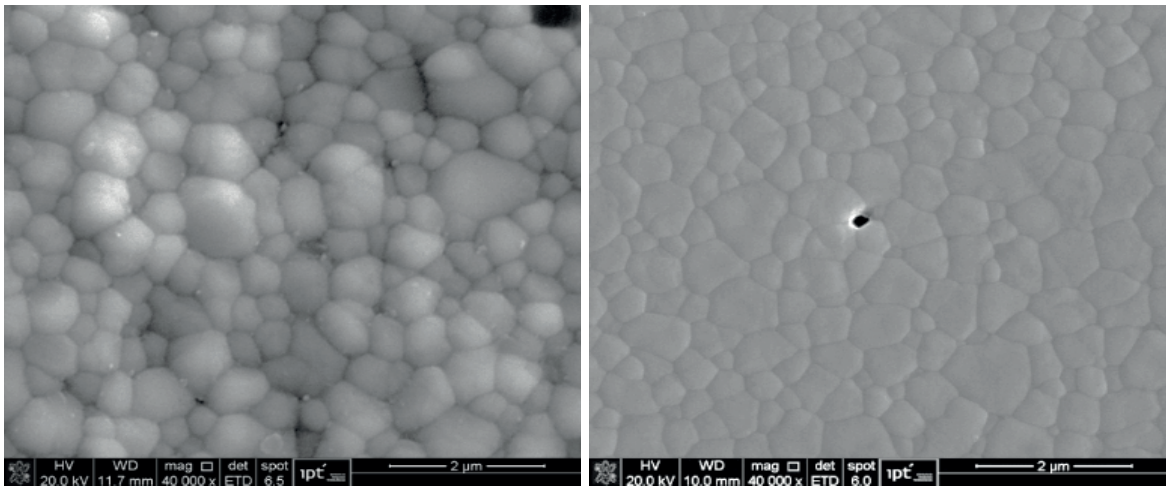

(a)

ZS0.0 (1500 °C)

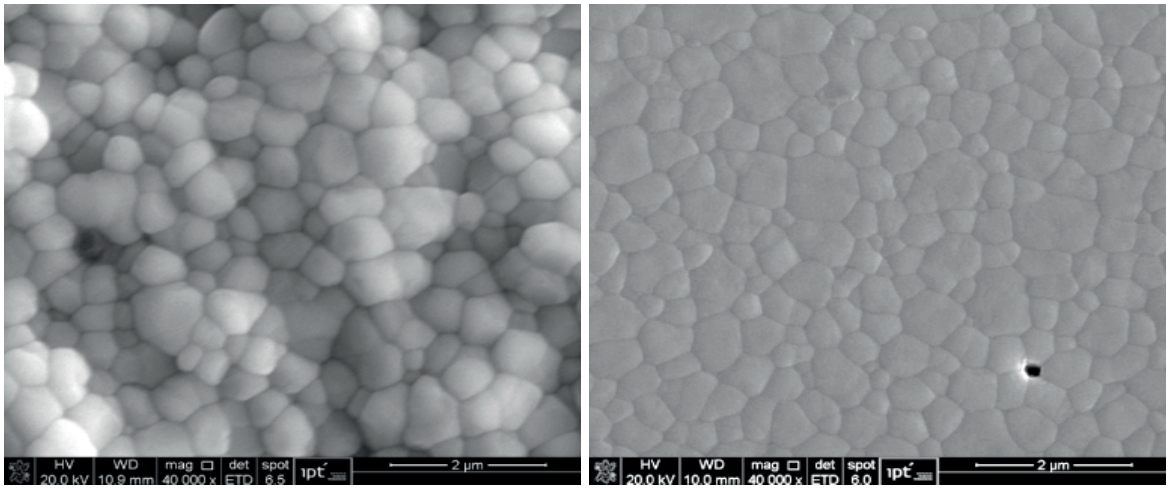

(b)

ZS0.8 (1500 °C)

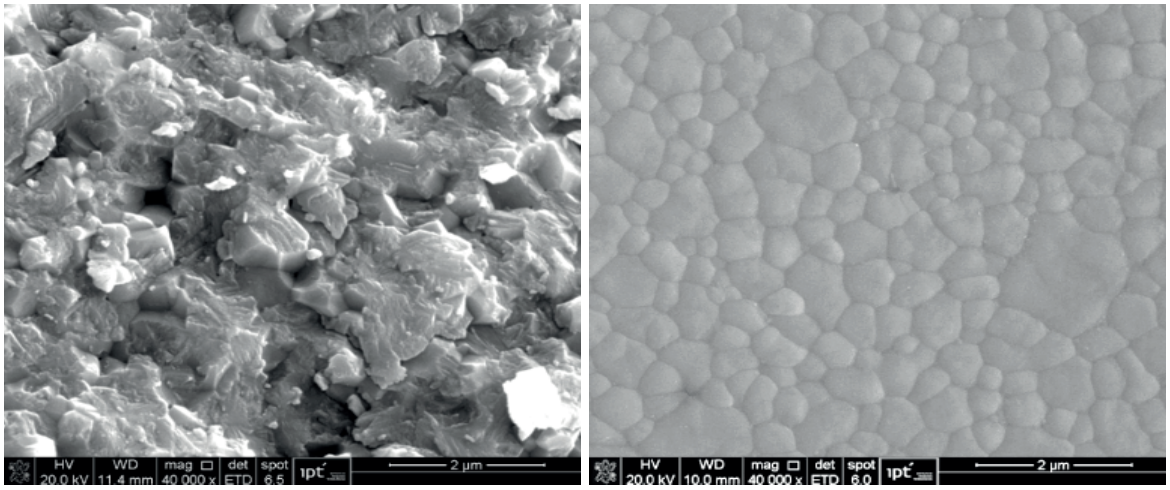

(c)

ZM0.8 (1500 °C)

Source: created by authors

A slight bias for lower densification of ZM0.8 samples (ground zirconia) was observed related to ZS0.0 and ZS0.8 (unground zirconia). The highest influence regarding grinding was observed in specimens processed at 1200 °C, with approximately 2.6 % difference in densification. At higher temperatures (1400 °C and 1500 °C), the difference is lower, around 1 % when considering the average value. Lopes (2009) reported similar densification values with those found in this study when sintering 3Y-TZP (Tosoh) in the range from 1400 °C to 1500 °C. The addition of 0.8 % wt of monoclinic Nb_2O_5 showed a very slight decrease in the densification of ungrounded TZ–3Y–E.

Figure 11 presents grain size as a function the temperature for the ZS0.0, ZS0.8 and ZM0.8 sintered compacts. It can be noted that the grain size for the samples heat-treated at 1200 °C does not show a significant difference. The same behavior was observed for the density of the compacts at this temperature. The medium grain size for the compacts obtained at 1400 °C and 1500 °C shows a slightly higher value and a heterogeneous distribution for the samples obtained with grounded zirconia. It can be concluded that the microstructure of the compacts obtained from the spray-dried powders, without grinding, seems to be formed by smaller and more uniform grains. Grain size is an important property for ceramics, because the smaller and homogeneous the grain size is, the higher the mechanical properties are. Some pores are observed in the micrographs since full densification was not reached. Santana et al. (2008) studied the sintering of the same stabilized zirconia powder with 8 % wt of Y_2O_3 atomized and non atomized and had obtained similar results regarding the grain shape and size.

Figure 11 – Grain size as a function of temperature for samples with TZ-3Y-E with (ZM0.8) and without grinding (ZS0.0 and ZS0.8)

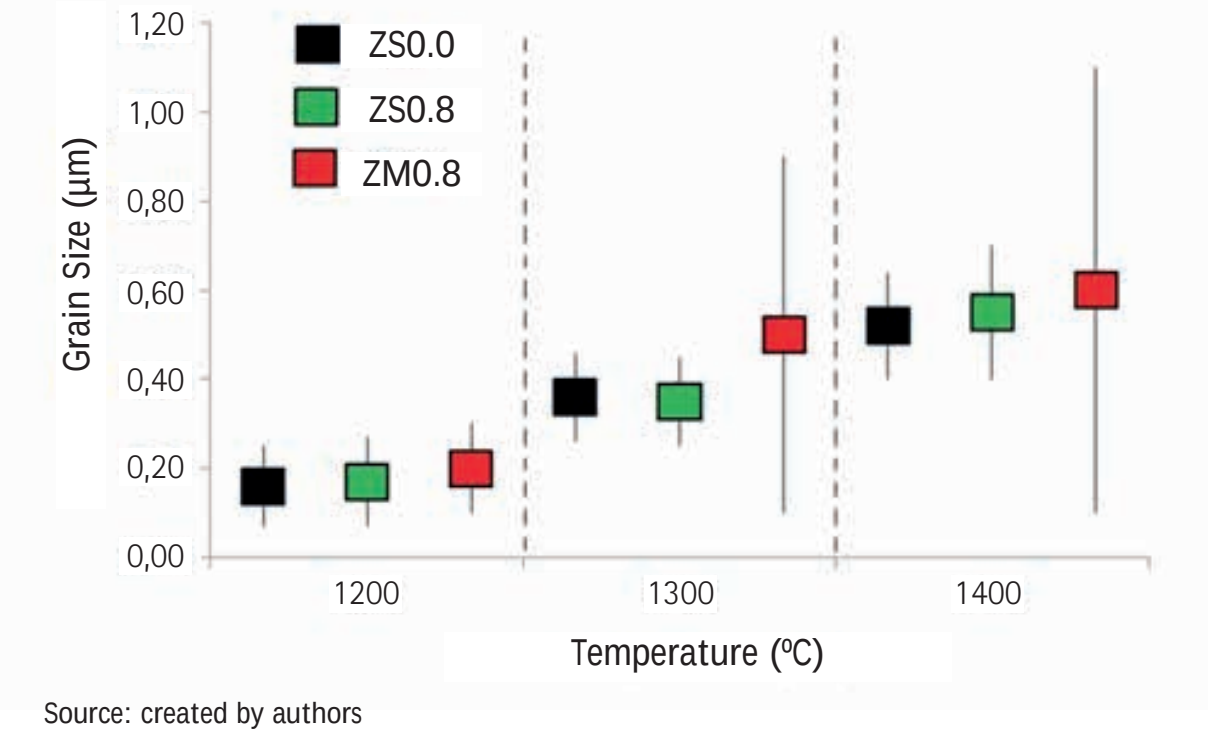

Source: created by authors

3.4 Scanning Electron Microscopy and X-Ray Diffraction

As mentioned before and shown in Figure 7, specimens with 2 wt% of Nb_2O_5 presents numerous cracks after heat treatment at 1400 °C for 3 h. Figure 12 shows the X-ray diffractograms of samples ZS0.0, ZS0.8 and ZS2.0.

Figure 12 – X-ray diffractograms of ZS0.0, ZS0.8, ZS2.0

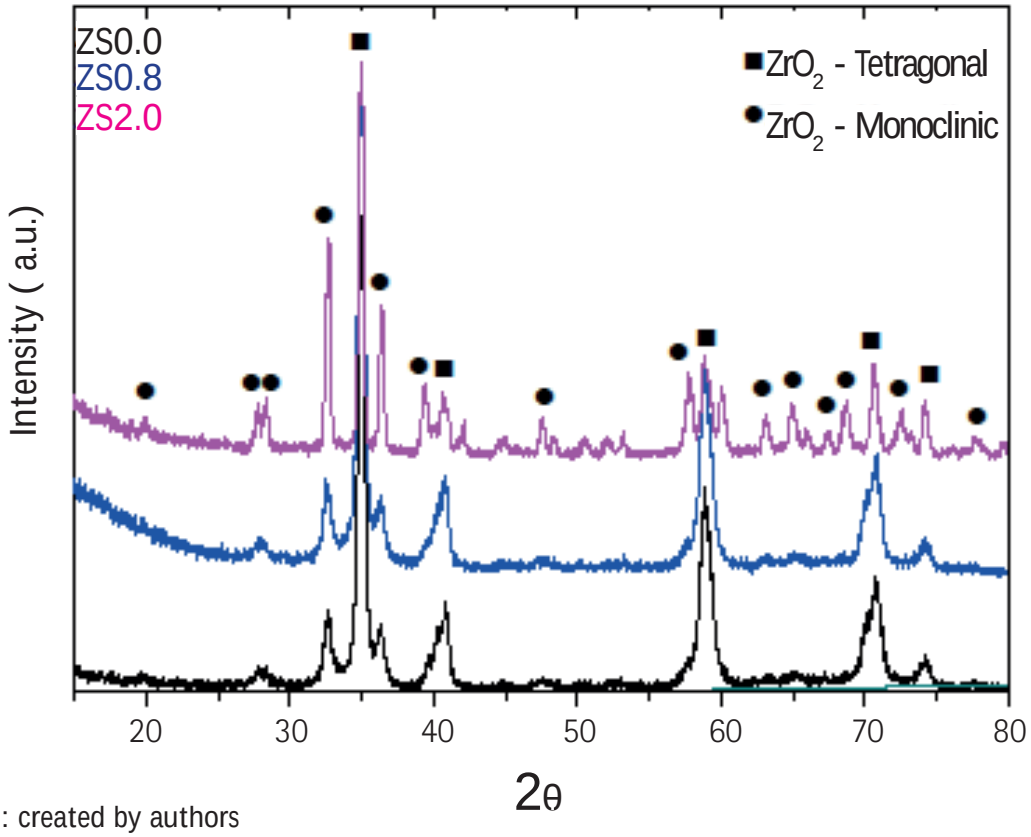

Source: created by authors

The diffractograms of ZS0.0 and ZS0.8 are almost identical in relation to the phases m-ZrO_2 and t-ZrO_2 and their relative intensities, indicating that the addition of 0.8 % wt of monoclinic Nb_2O_5 did not result in the destabilization of zirconia. On the other hand, the addition of 2.0 % wt of monoclinic niobium pentoxide proved to be inadequate for producing ceramics for technical applications, due to the transformation of phase m→t-ZrO_2 resulting in the high formation of cracks and fragmentation of the specimen. The results obtained in this study are similar to those obtained by Golieskardi (2014), which used a maximum of 1 % wt of Nb_2O_5 (0.70 % mol). In Kim's work (1990) it is reported that only above 1.5 % wt (3 % mol) it was difficult to obtain a pure tetragonal phase. It is important to highlight that in the mentioned studies the polymorph of Nb_2O_5 was not reported, and Kim (1990) used the coprecipitation method to prepare the mixture of oxides.

Figure 13 shows a scanning electronic micrograph image of the fractured surface of ZS2.0 sample. Intergranular fracture (crack along the grain boundaries) and intragranular fracture (cracks within the grains) can be observed, showing the severe stress due to the m→t-ZrO_2 transformation, causing the fracture of the sample.

Figure 13 – Micrograph obtained by SEM from the ZS2.0 compact obtained at 1400 ºC for 3 h. Arrows indicate cracks

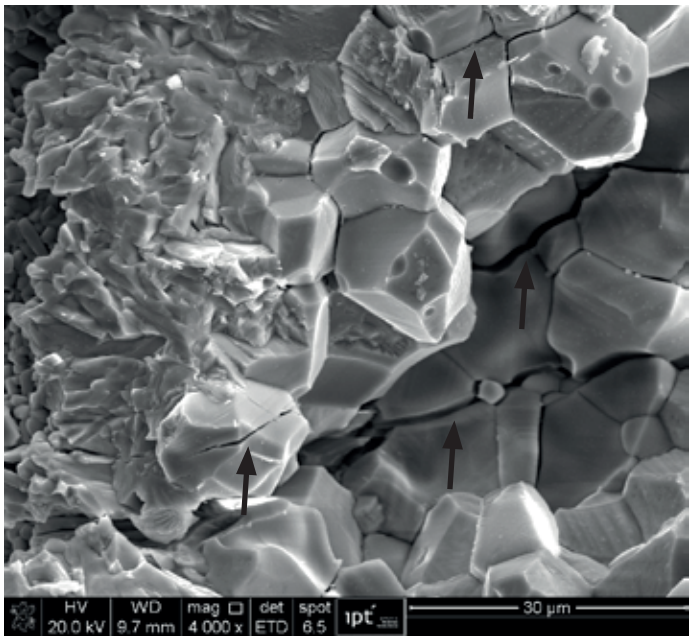

Source: created by authors

An interesting fact observed in the ZS2.0 sample was the presence of rounded regions (Figure 14) with morphologies differentiated from those observed in Figures 8 to 10. As the niobium pentoxide content was a maximum of 2 % wt, it was not possible to identify it using X-ray diffraction. However, using Raman spectroscopy, which is a technique that allows the analysis of specific regions in the sample, the monoclinic ZrO_2 spectrum was observed (Figure 15). A spectrum that had neither relation with the monoclinic and tetragonal zirconia phases nor with the monoclinic and orthorhombic niobium pentoxide phases was also obtained (Figure 16). Thus, a standard analysis of the compound $Zr_6Nb_2O_{17}$ ($6ZrO_2.Nb_2O_5$) was performed, as shown in the diffractograms of Figure 17. It was found that the Raman spectrum of a region similar to that presented in Figure 16 is equal to the phase $Zr_6Nb_2O_{17}$. It can be concluded that the addition of 2 % wt of monoclinic Nb_2O_5 resulted in the destabilization of the tetragonal phase for TZ–3Y-E and in the solid-state reaction of ZrO_2 and Nb_2O_5, forming zirconium niobate. The fact that it is a rounded region suggests that niobate formed into granules that were not destroyed during the uniaxial compaction process.

Figure 14 – Micrograph obtained by SEM of a small region (~ 90 µm) of ZS2.0 sample heat-treated at 1400 ºC for 3 h

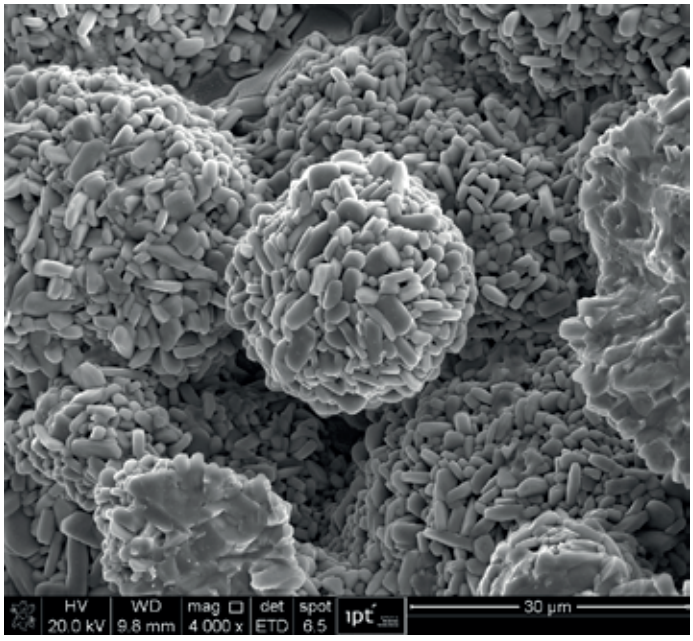

Source: created by authors

Figure 15 – Raman spectrum of the compact ZS2.0 treated at 1400 ºC for 3 h

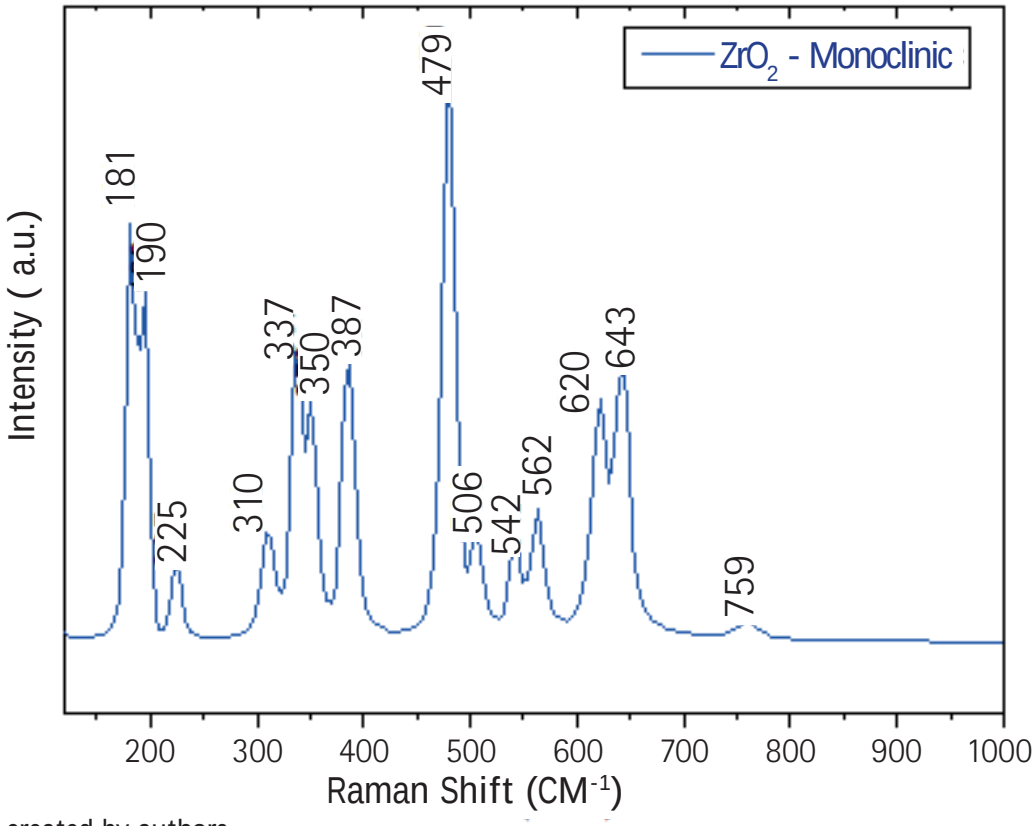

Source: created by authors

Figure 16 – Raman spectrum of the compact ZS2.0 treated at 1400 ºC for 3 h, compared with standard Zr_6Nb2O_{17}

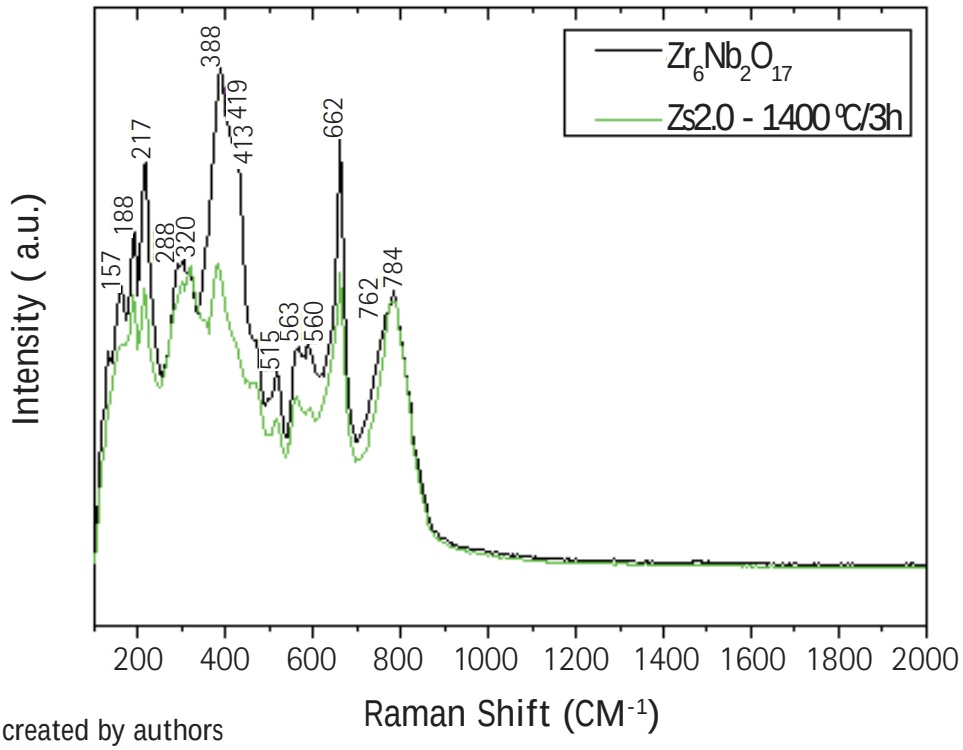

Source: created by authors

Figure 17 – X-ray diffractograms of zirconium niobate (Zr_6Nb2O_{17})

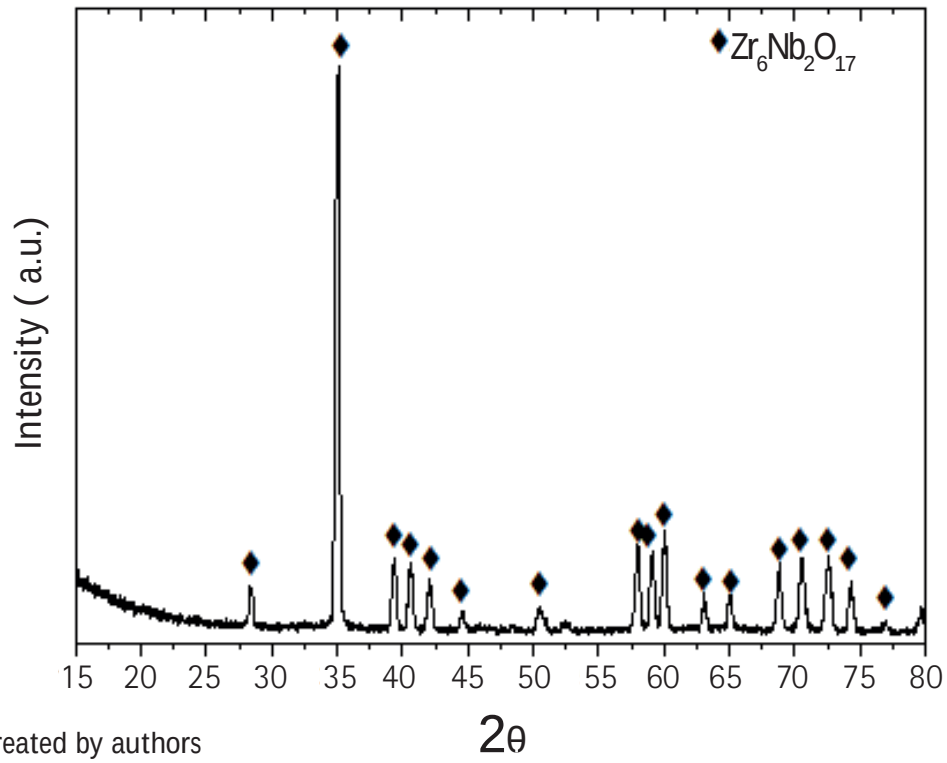

Source: created by authors

Several authors (JIN; GAO; KAN, 2002; RAI et al., 2017; KIM, 1990; KIM et al., 1998) reported that replacing Zr^{4+} for Y^{3+} in ZrO_2 results in the formation of oxygen vacancy, as represented below (Equation 2):

$$Y_2O_3 \xrightarrow{ZrO_2} 2Y'_{Zr} + V_O^{\cdot\cdot} + 3O_O \qquad (2)$$

where Y'_{Zr} and Vö represent Y^{3+} replacing Zr^{4+} in the crystalline reticle of zirconia and oxygen vacancy, respectively. The concentration of oxygen vacancy predominantly influences the stability of t-ZrO_2 in Y-TZP. When Y_2O_3 and Nb_2O_5 are added to zirconia, there is the elimination of oxygen vacancies, due the charge compensation between Y^{3+} and Nb^{5+} which can be represented by (KIM et al., 1998) (Equation 3):

$$Y_2O_3 + Nb_2O_5 \xrightarrow{ZrO_2} 2Y'_{Zr} + 2Nb^{\cdot}_{Zr} + 8O_O \qquad (3)$$

Thus, the stabilization of zirconia is compromised, demonstraiting that it is possible to add low niobium pentoxide content to the stabilizes zrconia with yttria in such a way as to obtain intact monolithic ceramics for technical applications.

4 Conclusions

Through this study, it is possible to conclude:

- *the addition of 0.8 % wt of monoclinic Nb_2O_5 in unground and ground TZ-3Y-E did not result in the destabilization of zirconia;*
- *there was observed a slight differences in the densification between TZ-3Y-E ground and non ground with 0.8 % wt of monoclinic Nb_2O_5, especially for compacts sintered at 1200 °C, and in the microstructure formed with smaller and homogeneous grain size distribution in the compacts obtained with non ground TZ-3Y-E;*
- *the addition of 2 wt% of monoclinic Nb_2O_5 in TZ-3Y-E proved to be ineffective at sintering, as it presented numerous cracks. This level of niobium pentoxide saturation in the sample caused the destabilization of the zirconia tetragonal and also resulted in the formation of $Zr_6Nb_2O_17$.*

5 References

BEJUGAMA, S.; PANDEY, A. K. Effect of Nb2O5 on sintering and mechanical properties of ceria stabilized zirconia. *Journal of Alloys and Compounds*, v. 765, p. 1049-1054, 2018.

BRITO, F. I. G.; MEDEIROS, K. F.; LOURENÇO, J. M. Um estudo teórico sobre a sinterização na metalurgia do pó. *Holos*, v. 3, p. 204-211, 2007.

CALLISTER, W. D. *Ciência e engenharia de materiais*: uma introdução. 9. ed. São Paulo: LTC Editora, 2016.

GOLIESKARDI M.; SATGUNAM, M.; RAGURAJAN, D. The influence of niobium pentoxide (Nb_2O_5) on the sintering behavior of yttria tetragonal zirconia polycrystal using two-step sintering (TSS) Method. *Australian Journal of Basic and Applied Sciences*, v. 8, n. 15, p. 59-63, 2014.

GUHA, J. P. Studies on niobium oxides and polymorphism of niobium pentoxide. *Transactions of the Indian Ceramic Society*, v. 28, n. 4, p. 97-101, 1969.

GUPTA, T. K.; BECHTOLD, J. H.; KUZNICKI, R. C.; CADOFF, L. H.; ROSSING, B. R. Stabilization of tetragonal phase in polycrystalline zirconia. *Journal of Materials Science*, v. 12, p. 2421-2426, 1977.

GUPTA, T. K.; LANGE, F. F.; BECHTOLD, J. H. Effect of stress-induced phase transformation on the properties of polycrystalline zirconia containing metastable tetragonal phase. J*ournal of Materials Science*, v. 13, p. 1464-1470, 1978.

HAYNES, W. M. (Ed.). *Handbook of chemistry and physics*. 95 ed. Boca Raton: CRC Press, 2014. Section 6-7, p. 1098.

HWANG, C. M. J.; CHEN, I. W. Effect of a liquid phase on superplasticity of 2-mol%-Y_2O_3-stabilized tetragonal zirconia polycrystals. *Journal of the American Ceramic Society*, v. 73, p. 1626-1632, 1990.

JIN, X.; GAO, L.; KAN, Y. M. Effects of Nb_2O_5 on the stability of t-ZrO2 and mechanical properties of ZTM. *Materials Letters*, v. 52, p. 10-13, 2002.

KIM, D. J. Effect of Ta_2O_5, Nb_2O_5, and HfO_2 alloying on the transformability of Y_2O_3-stabilized tetragonal ZrO_2. *Journal of the American Ceramic Society*, v. 73, 1, p. 115-120, 1990.

KIM, D. J.; JUNG, H. J.; JANG, J. W.; Lee H. L. Fracture toughness, ionic conductivity, and low-temperature phase stability of tetragonal zirconia codoped with yttria and niobium oxide. J*ournal of the American Ceramic Society*, v. 81, n. 9, p. 2309–2314, 1998.

KIMURA, N., ABE, S.; MORISHITA, J.; OKAMURA, H. Low temperature sintering of Y-TZP and Y-TZP-Al_2O_3 composites with transitional metal oxide additives. In: SOMIYA, S. (Ed.). *Sintering 88*. [.S.l.]: Elsevier Applied Science, 1988. v. 2, p. 1142-1148.

LOPES, O. F.; MENDONÇA, V. R.; SILVA, F. B. F.; PARIS, E. C.; RIBEIRO, C. Óxidos de nióbio: uma visão sobre a síntese do Nb2O5 e sua aplicação em fotocatálise heterogênea. *Química Nova*, v. 38, n. 1, p. 106-117, 2015.

LOPES, R. J. *Efeitos da temperatura de sinterização nas propriedades mecânicas e na resistência ao envelhecimento de cerâmicas de zircônia (3Y-TZP) para aplicações dentárias*. 2009. 78 f. Dissertação (Mestrado em Processos Industriais) – Instituto de Pesquisas Tecnológicas do Estado de São Paulo, São Paulo, 2009.

PIRALEK, B.; PELCZARSKA, A. J.; SZCZYGIEL, I. Characterization of niobium (V) oxide received from different sources. *Journal of Thermal Analysis and Calorimetry*, v. 130, p. 77-83, 2017.

RAI, K. A.; SINGH, R. P.; SINGH, S.; JAISWAL, A.; OMAR, S. Phase stability and ionic conductivity of cubic xNb_2O_5-(11-x)Sc_2O_3-ZrO_2 ($0 \leq x \leq 4$). *Journal of Alloys and Compounds*, v. 703, p. 643-651, 2017.

RAMESH, S.; GILL, C. Environmental degradation of CuO-doped Y-TZP ceramics. Ceramics International, v. 27, n. 6, p. 705-711, 2001.

RAN, S.; WINNUBST, A. J. A.; KOSTER, H.; DE VEEN, P. J.; BLANK, D. H. A. Sintering behaviour and microstructure of 3Y-TZP+8% CuO nano-powder composite. *Journal of European Ceramic Society*, v. 27, n. 2-3, p. 683-687, 2007.

RODDATIS, V. V.; SU, D. S.; BECKMANN, E.; JENTOFT, F. C.; BRAUN, U.; KRÖHNERT, J.; SCHLÖGL, R. The structure of thin zirconia films obtained by self-assembled monolayer mediated deposition: TEM and HREM study. *Surface and Coatings Technology*, v. 151-152, p. 63-66, 2002.

SANTANA, L. P.; LAZAR, D. R. R.; YOSHITO. W. K.; USSUI. V.; PASCHOAL. J. O. A. Spray-dried YSZ ceramic powders: Influence of slurry stability on physical characteristics of agglomerates. *Materials Science Forum*, v. 591-593, p. 465-470, 2008.

YOSHIMURA, H. N.; MOLISANI, A. L.; NARITA, N. E.; GONÇALVES, M. P.; CAMPOS, M. F. Zircônia parcialmente estabilizada de baixo custo produzida por meio de mistura de pós com aditivos do sistema MgO-Y_2O_3-CaO. *Cerâmica*, v. 53, p. 116-132, 2007.

DOI 10.34033/2526-5830-v4n13-4